iScience

CellPress
OPEN ACCESS

Article

Prdm14 promotes mouse ESC self-renewal and PGCLC specification through enhancement of Stat3 activity

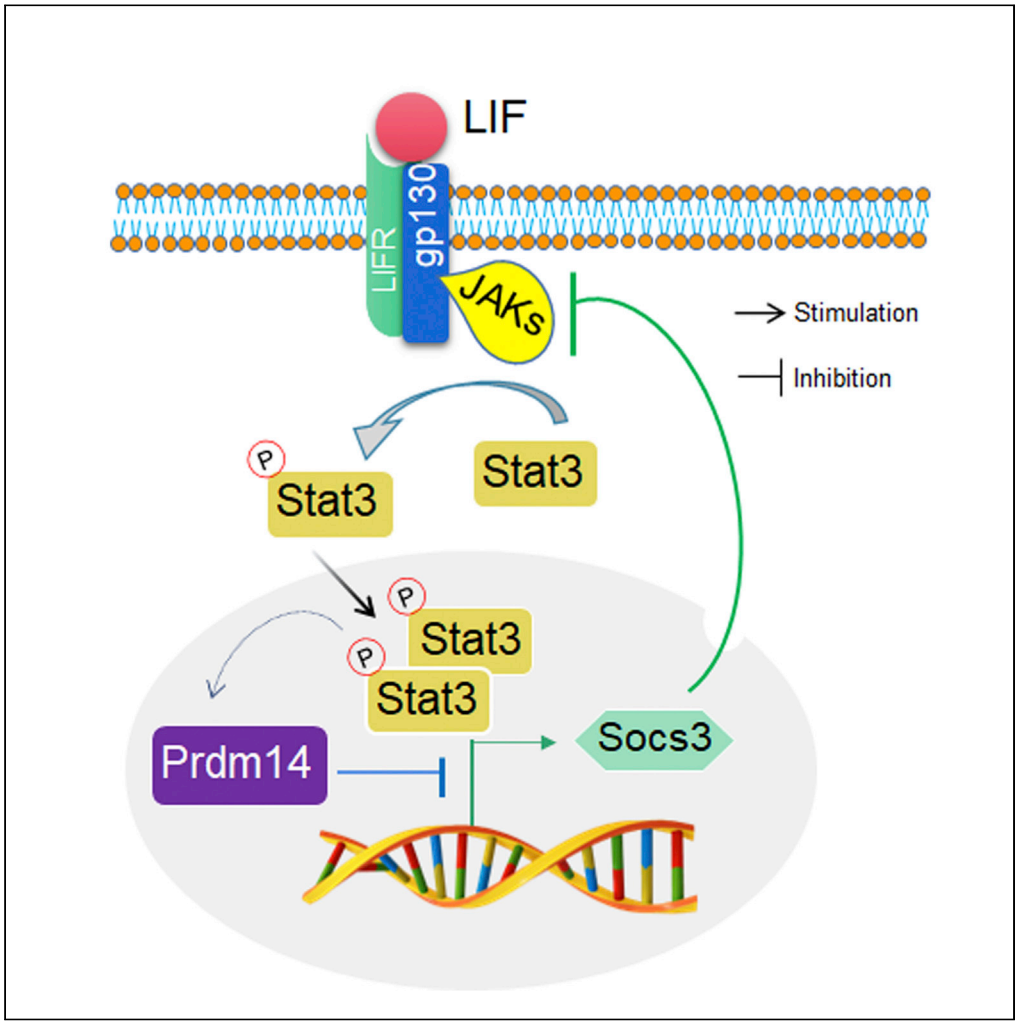

Yuting Li, Ziqiong Yang, Xiangfen Li, ..., Bing Li, Xiaoxiao Wang, Shou-Dong Ye

stemxi@126.com (X.W.)
shdye@126.com (S.-D.Y.)

Highlights

Prdm14 increases the phosphorylation of Stat3 by decreasing Socs3 transcription

Socs3 upregulation impairs *Prdm14*-mediated ESC maintenance and PGCLC formation

Stat3 inhibition represses *Prdm14*-mediated ESC self-renewal and PGCLC specification

Li et al., iScience *25*, 105293
November 18, 2022
https://doi.org/10.1016/j.isci.2022.105293

iScience

CellPress
OPEN ACCESS

Article

Prdm14 promotes mouse ESC self-renewal and PGCLC specification through enhancement of Stat3 activity

Yuting Li,[1,3] Ziqiong Yang,[1,3] Xiangfen Li,[1,3] Yang Yu,[1] Xiaofeng Li,[1] Peng Chen,[1] Bing Li,[1] Xiaoxiao Wang,[2,*] and Shou-Dong Ye[1,4,*]

SUMMARY

Prdm14 plays an important role in the maintenance of mouse embryonic stem cell (mESC) pluripotency and the specification of primordial germ cells (PGCs). However, the mechanism downstream of Prdm14 is still not fully understood. Here, using high-throughput sequencing, chromatin immunoprecipitation, and luciferase reporter assays, we show that Prdm14 directly binds to the promoter of *Socs3* and represses its transcription to increase the phosphorylation level of Stat3 protein, a critical downstream effector of LIF. Therefore, ectopic expression of *Socs3* is able to decrease the ability of Prdm14 to promote mouse mESC self-renewal and PGC-like cell generation. As expected, similar phenotypes were observed in *Prdm14*-transfected mESCs after knockdown of *Stat3* transcripts or treatment with a pan-inhibitor of JAKs, positive modulators of the LIF/Stat3 signaling pathway. These data will facilitate a better understanding of the regulatory network governing ESC identity and germ cell development.

INTRODUCTION

Embryonic stem cells (ESCs) isolated from the inner cell mass of the preimplantation blastocyst have unlimited ability to proliferate and generate different types of adult cells (Huang et al., 2015). Mouse ESCs (mESCs) were first established in 1981 (Evans and Kaufman, 1981; Martin, 1981). They can be maintained in serum-containing medium on feeder cells, and the latter can be replaced by leukemia inhibitory factor (LIF) (Smith et al., 1988; Williams et al., 1988). LIF binds to the LIF receptor and glycoprotein 130 (gp130) to form a heterodimeric complex and then phosphorylates the JAKs (Janus kinases) bound to the gp130 receptor. The phosphorylated JAKs recruit signal transducers and activators of transcription (Stat3) and phosphorylate the tyrosine residue of Stat3 at site 705 (Niwa et al., 1998). Two phosphorylated Stat3 proteins form homodimers and enter the nucleus to stimulate the expression of downstream target genes (Niwa et al., 1998), such as *Socs3* (Li et al., 2005), *Klf4* (Hall et al., 2009), *Gbx2* (Tai and Ying, 2013), *Sp5* (Ye et al., 2016), and *Tfcp2l1* (Martello et al., 2013; Ye et al., 2013). Overexpression of each gene can partially recapitulate the self-renewal-promoting effect of the LIF/Stat3 signaling pathway, except for *Socs3* (Hall et al., 2009; Li et al., 2005; Martello et al., 2013; Tai and Ying, 2013; Ye et al., 2013). Socs3 is a potent inhibitor of JAKs (Sasaki et al., 1999), and can directly inhibit the catalytic activity of three JAKs, JAK1, JAK2, and TYK2, with noncompetitive kinetics by blocking substrate binding (Babon et al., 2012; Kershaw et al., 2013). Therefore, Socs3 functions as a negative regulator of the LIF/Stat3 signaling pathway and will block self-renewal of ESCs directed by LIF when overexpressed (Chambers and Smith, 2004; Li et al., 2005). In addition to maintaining the stemness of stem cells, LIF/Stat3 signaling is also crucial for the induction of primordial germ cell-like cells (PGCLCs) *in vitro* (Hayashi et al., 2011). The addition of LIF is able to robustly promote the generation of PGCLCs from mESC-derived epiblast-like cells (EpiLCs) in combination with other cytokines, such as bone morphogenetic protein 4 (BMP4), stem cell factor (SCF), and epidermal growth factor (EGF) (Hayashi et al., 2011). Thus, the LIF/Stat3 signaling pathway has multiple characteristics when ESCs are in different niches.

Similar to the function of LIF/Stat3 signaling, the transcription factor PR domain containing 14 (Prdm14) also plays an important role in maintaining the stemness of mESCs and inducing PGCLCs from pluripotent stem cells (Nakaki et al., 2013; Okashita et al., 2015). The transcript of *Prdm14* is highly expressed in the inner cell mass of the blastocyst but is rapidly decreased in the epiblast at the postimplantation stage in mice (Yamaji

[1]Center for Stem Cell and Translational Medicine, School of Life Sciences, Anhui University, Hefei, Anhui 230601, China

[2]Core Facility Center, The First Affiliated Hospital of USTC (Anhui Provincial Hospital), Hefei, Anhui 230001, China

[3]These authors contributed equally

[4]Lead contact

*Correspondence: stemxi@126.com (X.W.), shdye@126.com (S.-D.Y.)

https://doi.org/10.1016/j.isci.2022.105293

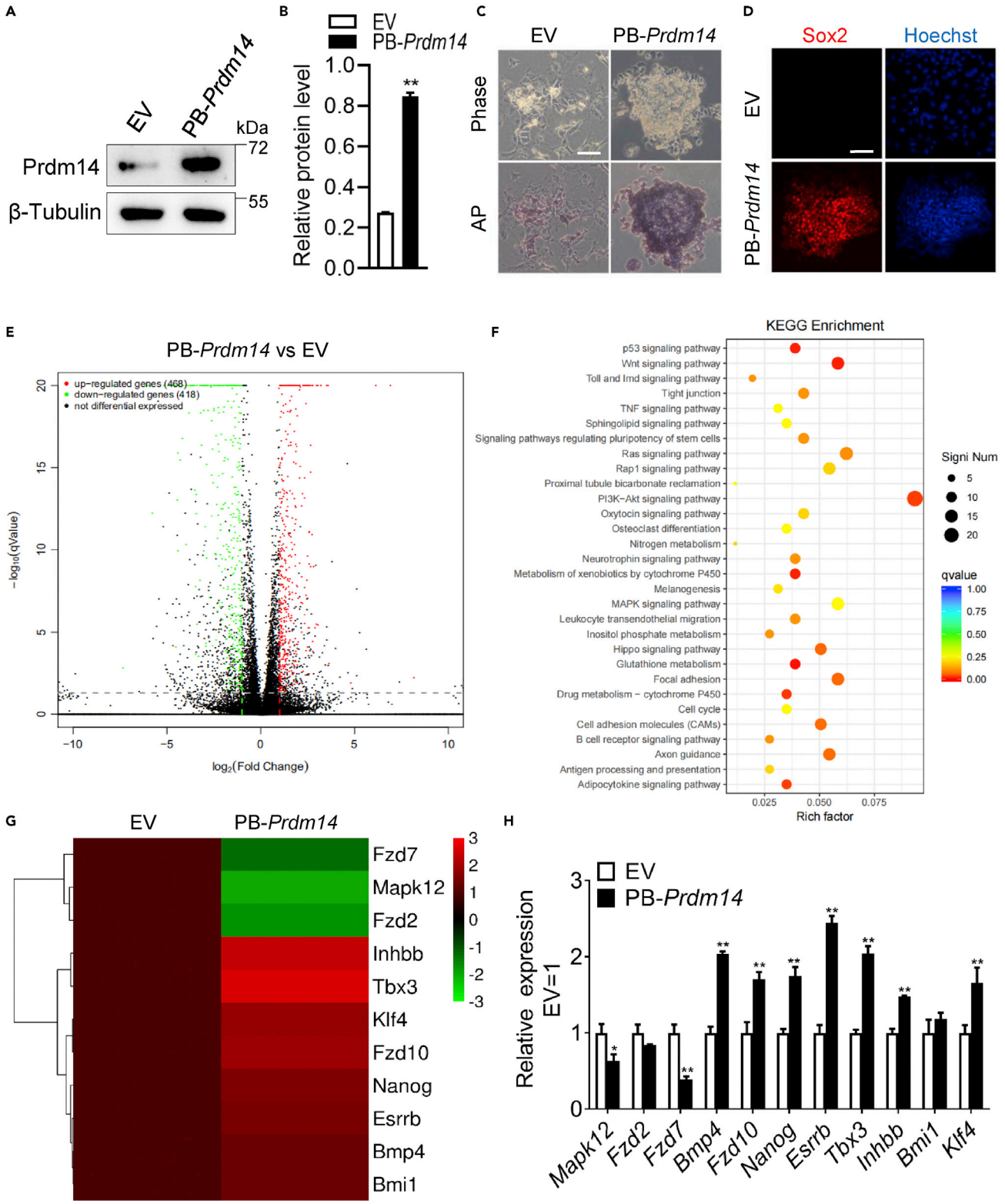

Figure 1. Investigation of the gene expression profile in *Prdm14*-overexpressing cells

(A) Western blot analysis of the total protein levels of Prdm14 in 46C mESCs transfected with EV or PB-*Prdm14* and cultured in LIF/serum conditioned medium.

Figure 1. *Continued*

(B) Densitometric analysis of the relative protein level of Prdm14 was performed with ImageJ software. Protein levels were normalized to β-Tubulin (N = 3 biological replicates). **p < 0.01 versus EV, as determined by Student's *t* test.

(C) Phase contrast images and alkaline phosphatase (AP) staining of EV and PB-*Prdm14* mESCs cultured in serum-containing medium without LIF for seven days. Bar,100 μM.

(D) Immunofluorescence staining of Sox2 in EV and PB-*Prdm14* mESCs treated without LIF for seven days. Bar,100 μM.

(E) Volcano map showing the differentially expressed genes regulated by PB-*Prdm14*.

(F) KEGG analysis of the DEGs regulated by PB-*Prdm14*.

(G) Heatmap showing the expression pattern of stem cell pluripotency-associated genes in EV- and PB-*Prdm14*-expressing cells. Genes were ranked at the level of a log2-fold change.

(H) qRT−PCR analysis of the expression levels of candidate genes regulated by PB-*Prdm14* in (G). The data are presented as the mean ± SD (N = 3 biological replicates). *p < 0.05, **p < 0.01 versus EV, as determined by Student's *t* test.

See also Figure S1 and Tables S1 and S3.

et al., 2008). Therefore, enforced expression of mouse *Prdm14* is sufficient to sustain the undifferentiated state and pluripotency of mESCs in the absence of LIF (Okashita et al., 2015). The associated molecular mechanisms may involve DNA methyltransferases- and ten-eleven translocation (Tet)-mediated active DNA demethylation and low Fgf/Mek/Erk signaling pathway activity (Okashita et al., 2015; Sim et al., 2017; Yamaji et al., 2013). Prdm14 inhibits its target genes largely by recruiting polycomb repressive complex 2 (PRC2), which mediates histone H3 lysine 27 trimethylation (H3K27me3) for gene repression (Margueron and Reinberg, 2011; Yamaji et al., 2013). In addition, Prdm14 has been identified as a key regulator of the differentiation of epiblasts into PGCLCs (Nakaki et al., 2013). *Prdm14* is specifically upregulated during primordial germ cell (PGC) specification from the epiblast and is required for the early development of PGCs *in vivo* (Yamaji et al., 2008). *In vitro*, constitutive expression of *Prdm14* alone is sufficient to direct mouse EpiLCs swiftly and efficiently into a PGC state (Nakaki et al., 2013). Although the ETO-family corepressor Mtgr1 tightly binds to the pre-SET/SET domains of Prdm14 and co-occupies its genomic targets in mESC maintenance and PGCLC formation (Nady et al., 2015), the transcriptional regulatory network downstream of Prdm14 is still not well understood.

To address this issue, we performed high-throughput sequencing and chromatin immunoprecipitation (ChIP) experiments and revealed that *Prdm14* directly inhibits *Socs3* transcription. Functional validation showed that *Prdm14* promotes mESC self-renewal and PGCLC generation, at least in part, by amplification of the LIF/Stat3 signaling pathway. These results connect Prdm14 with the activation of LIF/Stat3, one important mechanism for the maintenance of mESC identity and the generation of PGCLCs.

RESULTS

Screening ESC self-renewal-associated genes downstream of *Prdm14*

Previously studies have shown that overexpression of *Prdm14* in mESCs was able to sustain the levels of self-renewal-associated genes but suppress the differentiation-related genes (Okashita et al., 2015; Yamaji et al., 2013). To confirm these results, we inserted Flag-tagged mouse *Prdm14* into the PiggyBac (PB) system and then transfected this construct into 46C mESCs. The protein level of Prdm14 was significantly increased (PB-*Prdm14*) (Figures 1A and S1A), and the total amount of Prdm14 protein after overexpression was approximately three times that of endogenous Prdm14 protein (Figure 1B). PB empty vector (EV) control and PB-*Prdm14*-expressing cells were then cultured in serum-containing medium in the absence of LIF. After seven days, PB-*Prdm14*-expressing cells retained typical features of mESC morphology, positive alkaline phosphatase (AP) activity, and high levels of the pluripotency marker Sox2, whereas EV control cells differentiated (Figures 1C, 1D, and S1B), suggesting that upregulation of *Prdm14* is sufficient to maintain the undifferentiated state of mESCs.

To explore the mechanism downstream of Prdm14, we performed high-throughput sequencing to screen the downstream genes in response to *Prdm14* upregulation. Compared with EV, *Prdm14* regulated many differentially expressed genes (DEGs) by 2-fold or greater; among them, 468 genes were upregulated and 418 genes were downregulated (Figure 1E). To further analyze the biological functions of these DEGs, Kyoto Encyclopedia of Genes and Genomes (KEGG) was performed. Specifically, we found that eleven candidate genes were enriched in the item "Signaling pathways regulating pluripotency of stem cells" (Figure 1F), including *Inhbb*, *Klf4*, *Fzd7*, *Tbx3*, *Nanog*, *Bmp4*, *Mapk12*, *Esrrb*, *Fzd10*, *Fzd2*, and *Bmi1* (Figure 1G). Meanwhile, quantitative real-time PCR (qRT−PCR) was carried out to validate their expression (Figure 1H). These data suggest that Prdm14 mediates the expression of many self-renewal and pluripotency genes in mESCs.

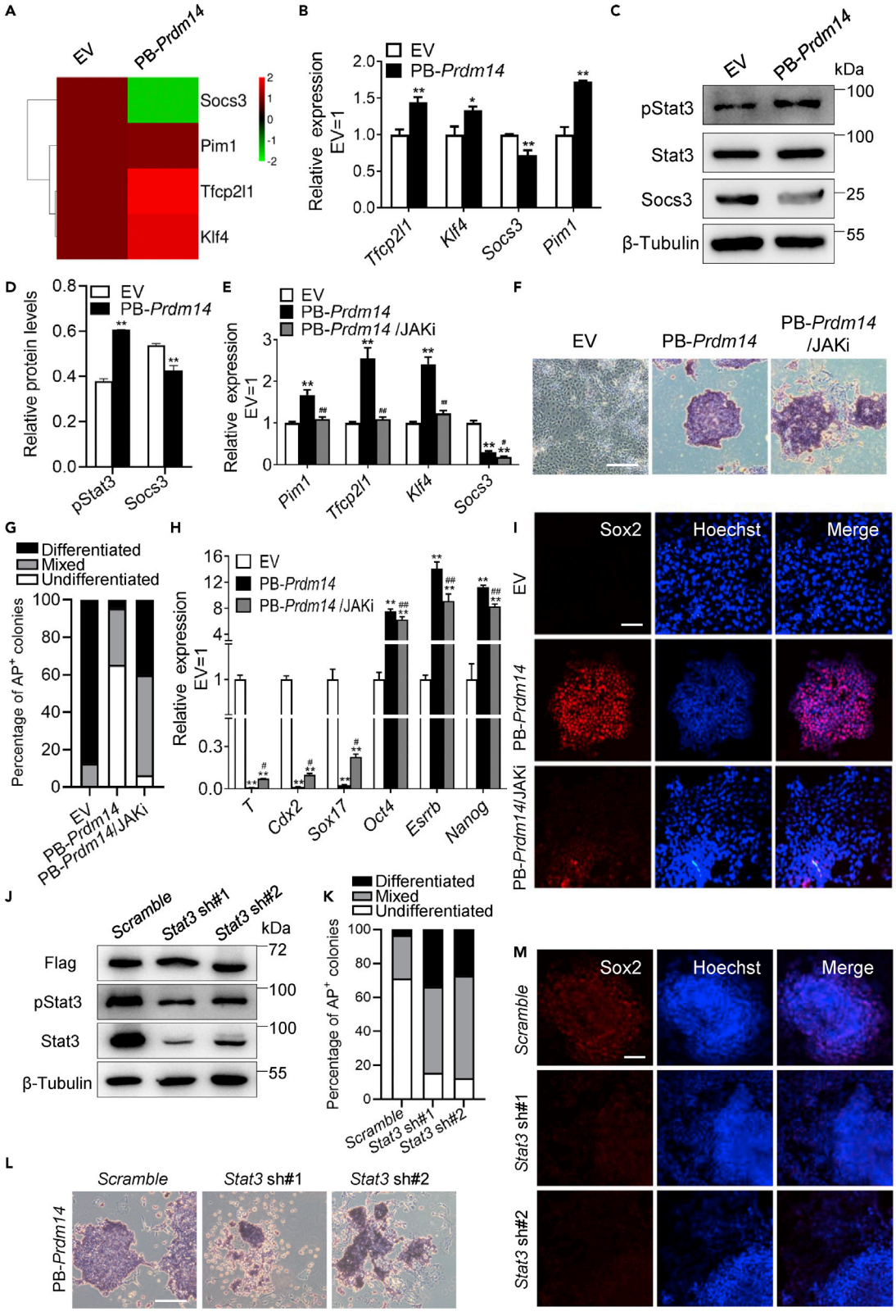
A
EV
PB-Prdm14
Socs3
Pim1
Tfcp2l1
Klf4
B
EV
PB-Prdm14
Relative expression EV=1
Tfcp2l1
Klf4
Socs3
Pim1
C
EV
PB-Prdm14
kDa
pStat3
Stat3
Socs3
β-Tubulin
100
100
25
55
D
EV
PB-Prdm14
Relative protein levels
pStat3
Socs3
E
EV
PB-Prdm14
PB-Prdm14 /JAKi
Relative expression EV=1
Pim1
Tfcp2l1
Klf4
Socs3
F
EV
PB-Prdm14
PB-Prdm14 /JAKi
G
Differentiated
Mixed
Undifferentiated
Percentage of AP+ colonies
EV
PB-Prdm14
PB-Prdm14/JAKi
H
EV
PB-Prdm14
PB-Prdm14 /JAKi
Relative expression EV=1
T
Cdx2
Sox17
Oct4
Esrrb
Nanog
I
Sox2
Hoechst
Merge
EV
PB-Prdm14
PB-Prdm14/JAKi
J
Scramble
Stat3 sh#1
Stat3 sh#2
kDa
Flag
pStat3
Stat3
β-Tubulin
72
100
100
55
K
Differentiated
Mixed
Undifferentiated
Percentage of AP+ colonies
Scramble
Stat3 sh#1
Stat3 sh#2
L
Scramble
Stat3 sh#1
Stat3 sh#2
PB-Prdm14
M
Sox2
Hoechst
Merge
Scramble
Stat3 sh#1
Stat3 sh#2

Figure 2. *Prdm14* depends on Stat3 activity to promote mESC self-renewal

(A) Heatmap showing the expression of direct targets of Stat3 isolated from the high-throughput sequencing of transcriptomes regulated by *Prdm14* upregulation. Genes were ranked according to the level of log2-fold change.

(B) qRT−PCR analysis of the expression of candidate genes in (A). The data are presented as the mean ± SD (N = 3 biological replicates). *p < 0.05, **p < 0.01 versus EV, as determined by Student's *t* test.

(C) Western blot analysis of Socs3, Stat3, and phospho-Stat3^{Y705} (pStat3) in 46C mESCs overexpressing EV or PB-*Prdm14*. β-Tubulin was used as a loading control.

(D) Densitometric analysis of the relative protein levels of pStat3 and Socs3 was performed with ImageJ software (C). Protein levels were normalized to β-Tubulin. **p < 0.01 versus EV, as determined by Student's *t* test.

(E) qRT-PCR analysis of the expression of Stat3 direct genes in EV- and PB-*Prdm14*-expressing cells cultured in serum-containing medium without LIF for 8 days in the presence or absence of 5 μM JAK inhibitor I (JAKi). The data are presented as the mean ± SD (N = 3 biological replicates). **p < 0.01 versus EV, $^{\#}$p < 0.05, $^{\#\#}$p < 0.01 versus PB-*Prdm14*, as determined by one-way ANOVA with Sidak's multiple comparisons test.

(F) AP staining of EV- and PB-*Prdm14*-expressing cells treated with or without JAKi for 8 days in the absence of LIF. Bar,100 μM.

(G) Quantification of AP-positive colonies in (F).

(H) qRT−PCR analysis of the expression levels of undifferentiated (*Oct4*, *Esrrb*, and *Nanog*) and differentiated genes (*T*, *Cdx2*, and *Sox17*) in EV- and PB-*Prdm14*-expressing cells treated with or without JAKi. The data are presented as the mean ± SD (N = 3 biological replicates). **p < 0.01 versus EV, $^{\#}$p < 0.05 versus PB-*Prdm14*, as determined by one-way ANOVA with Sidak's multiple comparisons test.

(I) Immunofluorescence of Sox2 in the indicated cells. Bar,100 μM.

(J) Western blot analysis of Flag, pStat3 and Stat3 protein levels in PB-*Prdm14*-expressing mESCs infected with *scramble* or *Stat3* shRNA lentiviruses.

(K) Quantification of AP-positive colonies in (L).

(L) AP staining of *Stat3* knockdown 46C mESCs overexpressing *Prdm14* in the absence of LIF. Bar,100 μM.

(M) Immunofluorescence staining of Sox2 in *Stat3* knockdown 46C mESCs overexpressing *Prdm14* and cultured in serum-containing medium without LIF for 8 days. Bar,100 μM.

See also Figures S2 and S3, Tables S2 and S3.

Inhibition of Stat3 activity impairs the self-renewal-promoting effect of *Prdm14*

Notably, we observed a significant change in the expression pattern of Stat3 targets among the *Prdm14*-medidated genes identified as DEGs through high-throughput sequencing, such as *Tfcp2l1*, *Klf4*, *Pim1*, and *Socs3* (Figure 2A). Interestingly, qRT−PCR analysis revealed that *Tfcp2l1*, *Klf4*, and *Pim1* were induced by *Prdm14*, while *Socs3* was significantly inhibited by *Prdm14* (Figure 2B). This phenomenon prompted us to speculate that ectopic expression of *Prdm14* might enhance the activity of the LIF/Stat3 signaling pathway by negatively regulating the transcription of *Socs3*. To validate this hypothesis, the total and phosphorylated Stat3 protein levels were examined. As expected, the total protein levels of Stat3 did not change, while the phosphorylation of tyrosine 705 of the Stat3 protein (pStat3) was increased by *Prdm14* overexpression, as shown by the Western blot and grayscale analysis results of the corresponding bands (Figures 2C and 2D). Next, to determine whether the LIF/Stat3 signaling pathway can mediate the function of Prdm14, JAK inhibitor I (JAKi), a pan-inhibitor of JAKs, was added to the culture medium of PB-*Prdm14*-expressing cells to block LIF/Stat3 signaling. As expected, JAK inhibitor I suppressed the expression of the Stat3 target genes *Pim1*, *Klf4*, *Tfcp2l1*, and *Socs3* induced by *Prdm14* (Figure 2E). After eight days, compared with PB-*Prdm14*-overexpressing cells, the addition of JAKi resulted in an obvious differentiation phenotype in *Prdm14*-overexpressing cells, characterized by decreased AP activity, low levels of the self-renewal and pluripotency markers *Oct4*, *Esrrb*, and *Nanog*, and high levels of the differentiation-associated genes *T*, *Cdx2*, and *Sox17* (Figures 2F–2I and S2). To confirm this observation, lentiviruses carrying two short hairpin RNAs (shRNAs) were used to infect 46C mESCs and silence mouse endogenous *Stat3* expression. Compared with cells transfected with the *scramble* control lentivirus, stable knockdown of *Stat3* transcript levels by approximately 70%–90% was observed at the mRNA level (Figure S3A). Consistently, the expression levels of the *Stat3* targets *Socs3*, *Klf4*, and *Tfcp2l1* were decreased (Figure S3A). The same number of *scramble* and *Stat3* shRNA-expressing mESCs was then seeded in serum-containing medium in the presence of LIF. After eight days, *Stat3* knockdown cells became flat and lost AP activity (Figures S3B and S3C), indicating that the suppression of *Stat3* is sufficient to abolish the self-renewal effect of LIF. Subsequently, we decreased *Stat3* transcripts in PB-*Prdm14*-expressing cells and observed that the total and phosphorylated Stat3 protein levels were obviously downregulated (Figure 2J). The decreased Stat3 activity inhibited the protein levels of Sox2 and AP activity (Figures 2K–2M and S3D). Overall, these results illustrate that Prdm14 partially depends on the activity of Stat3 to maintain mESC stemness.

Ectopic expression of *Socs3* disrupts the function of *Prdm14* in promoting mESC self-renewal

As a direct target of the LIF/Stat3 signaling pathway, the transcription of *Socs3* could be rapidly induced by short-term stimulation with LIF (Figures 3A and S4). Meanwhile, we noted that the transcript of *Prdm14* was

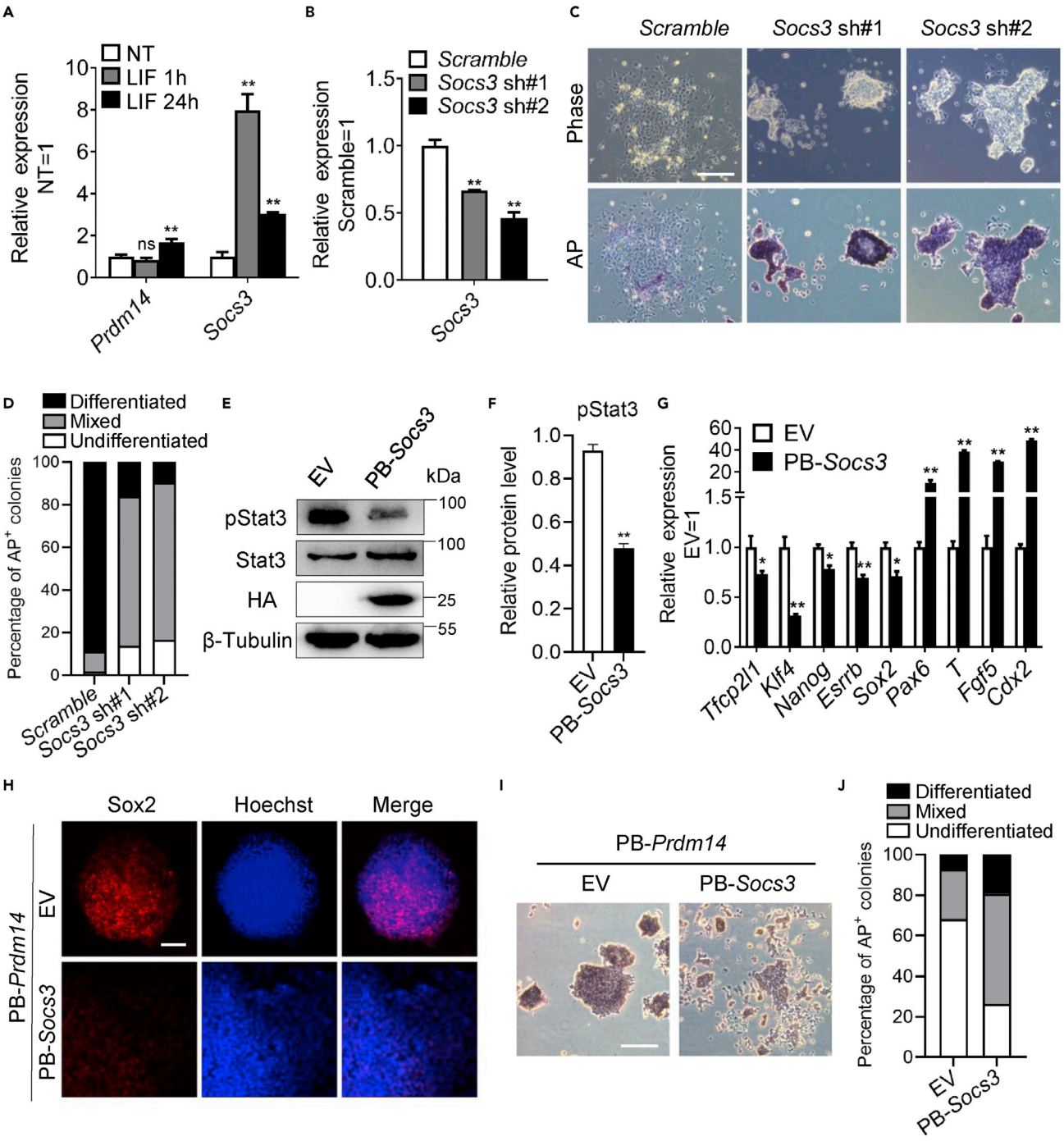

Figure 3. Upregulation of *Socs3* inhibits the self-renewal-promoting effect of *Prdm14*

(A) qRT–PCR analysis of the expression levels of *Prdm14* and *Socs3* in 46C mESCs cultured in serum-containing medium treated with LIF for 1 h or 24 h. The data are presented as the mean ± SD (N = 3 biological replicates). *p < 0.05, **p < 0.01 versus NT. NT, no treatment, as determined by one-way ANOVA with Dunnet's multiple comparisons test. ns: nonsignificant.

(B) qRT–PCR analysis of *Socs3* transcripts in 46C mESCs infected with *scramble* or *Socs3* shRNA lentiviruses. The data are presented as the mean ± SD (N = 3 biological replicates). **p < 0.01 versus scramble, as determined by one-way ANOVA with Dunnet's multiple comparisons test.

(C) AP staining of *scramble* and *Socs3* shRNA 46C mESCs cultured in serum-containing medium without LIF for eight days. Bar,100 μM.

(D) Quantification of AP-positive colonies in (C).

(E) Western blot analysis of HA, Stat3, and pStat3 in PB-*Prdm14*-expressing mESCs overexpressing EV or HA-tagged *Socs3*. β-Tubulin was used as a loading control.

Figure 3. *Continued*

(F) Densitometric analysis of the relative protein levels of pStat3 was performed with ImageJ software (E). Protein levels were normalized to β-Tubulin. **p < 0.01 versus EV, as determined by Student's *t* test.

(G) qRT−PCR analysis of the expression of undifferentiation (*Sox2*, *Nanog*, *Klf4*, *Esrrb*, and *Tfcp2l1*) and differentiation-associated genes (*T*, *Pax6*, *Cdx2*, and *Fgf5*) in PB-*Prdm14*-expressing mESCs overexpressing EV or HA-tagged *Socs3*. The data are presented as the mean ± SD (N = 3 biological replicates). *p < 0.05, **p < 0.01 versus EV, as determined by Student's *t* test.

(H and I) Immunofluorescence staining of Sox2 and AP staining of PB-*Prdm14*-expressing mESCs overexpressing EV or HA-tagged *Socs3* and cultured in serum-containing medium without LIF treatment for eight days. Bar, 100 μM.

(J) Quantification of AP-positive colonies in (I).

See also Figures S4 and S5 and Tables S1–S3.

higher in mESCs treated with LIF for 24 h than in untreated cells, whereas short-term treatment with LIF for 1 h failed to upregulate *Prdm14* (Figure 3A), indicating that *Prdm14* is downstream of Stat3 but is not a direct target of Stat3. We next decreased *Socs3* expression levels using two specific shRNA lentiviruses (Figure 3B). As a negative regulator of LIF/Stat3 signaling, knockdown of *Socs3* was capable of delaying mESC differentiation in the absence of LIF for eight days compared with *scramble* control cells (Figures 3C, 3D, and S5A). To investigate the direct association between Socs3 and Prdm14, HA-tagged *Socs3* (HA-*Socs3*) and empty vector EV were transduced into PB-*Prdm14*-expressing 46C mESCs (Figure 3E). Western blot analysis showed that overexpression of *Socs3* decreased the phosphorylation levels of $Stat3^{Y705}$ (Figures 3E and 3F). After culturing in serum-containing medium without the addition of LIF, HA-*Socs3*/PB-*Prdm14*-coexpressing mESCs became flat, exhibited weaker AP activity, and displayed lower levels of self-renewal and pluripotency markers (*Sox2*, *Nanog*, *Klf4*, *Esrrb*, and *Tfcp2l1*) but higher levels of differentiation-associated genes (*T*, *Pax6*, *Cdx2*, and *Fgf5*) than EV/PB-*Prdm14*-expressing cells in the absence of LIF for eight days (Figures 3G–3J and S5B), while EV/PB-*Prdm14*-expressing cells retained typical features of mESCs (Figures 3G–3J and S5B).Together, these results suggest that upregulation of *Socs3* can impair the *Prdm14*-induced resistance of mESCs to differentiation.

Prdm14 directly suppresses the expression of *Socs3*

Overexpression of *Prdm14* not only repressed *Socs3* expression (Figures 2A and 2B) but also inhibited the effect of LIF on *Socs3* induction (Figure S6). To further examine whether *Socs3* is a direct target of *Prdm14* and is suppressed by *Prdm14*, we carried out another four approaches. First, *Prdm14* transcripts were decreased by RNAi (*Prdm14* sh#1 and *Prdm14* sh#2). Knockdown of *Prdm14* enhanced *Socs3* expression, compared with *scramble* control cells (Figure 4A). Second, one *Prdm14* gene inducible cell line (i-*Prdm14*) was established using the PB-TETON system, in which exogenous *Prdm14* could be efficiently induced when treated with doxycycline (Dox). Short-term treatment with Dox for different times increased *Prdm14* expression (Figure 4B). Meanwhile, we observed that *Socs3* transcription was suppressed, while the levels of phosphorylation of Stat3 increased, when compared with untreated cells (Figures 4B and S7A–S7C). Third, to investigate whether the transcription of *Socs3* is directly regulated by Prdm14, we used the HOCOMOCO website (https://hocomoco11.autosome.ru/), which toward a complete collection of transcription factor binding models for humans and mice, identified via large-scale ChIP-Seq analysis (Kulakovskiy et al., 2018), to analyze the consensus binding motifs of Prdm14 (Figure 4C) and predicted two potential binding sites within *Socs3* promoter regions (from −4000 to +20). Motif 1 is located at −3681∼-3666, and motif 2 is located at −1626∼-1611. Thereafter, we performed chromatin immunoprecipitation (ChIP) in Flag-tagged *Prdm14*-expressing 46C mESCs with a Flag antibody and found that motif 1 had a significant enrichment ratio (Figure 4D). Finally, to confirm the *Prdm14*-mediated direct suppression of *Socs3*, we transfected reporter vectors that drive the expression of luciferase under the control of *Socs3* promoter fragments (PGL6-*Socs3*), containing wild-type motif 1 (WT) or mutated motif 1 sequences (Mut) with or without PB-*Prdm14* (Figure 4E). Under these conditions, we observed that upregulation of *Prdm14* decreased the luciferase activity driven by $Socs3^{WT}$ compared with PGL6-$Socs3^{WT}$ only transfected cells (Figure 4F). Nevertheless, PGL6-$Socs3^{Mut}$ transfectants had stronger luciferase activity than PGL6-$Socs3^{WT}$-expressing cells in the presence of *Prdm14* overexpression (Figure 4F). Taken together, these data indicate that Prdm14 directly binds to and inhibits Socs3 transcription. Interestingly, we noted that upregulation of *Prdm14* enhanced the level of H3K27me3 (Figure S8A) and further promoted H3K27me3 to bind more DNA fragments located at the −3734∼-3612 position of the Socs3 promoter (Figure S8B).

Overexpression of *Socs3* inhibits the role of *Prdm14* in inducing PGCLC specification

Prdm14 has well-characterized roles in promoting PGC specification *in vivo* and *in vitro* (Nakaki et al., 2013; Yamaji et al., 2008). Therefore, we wanted to examine whether Socs3 impacts *Prdm14*-mediated PGCLC

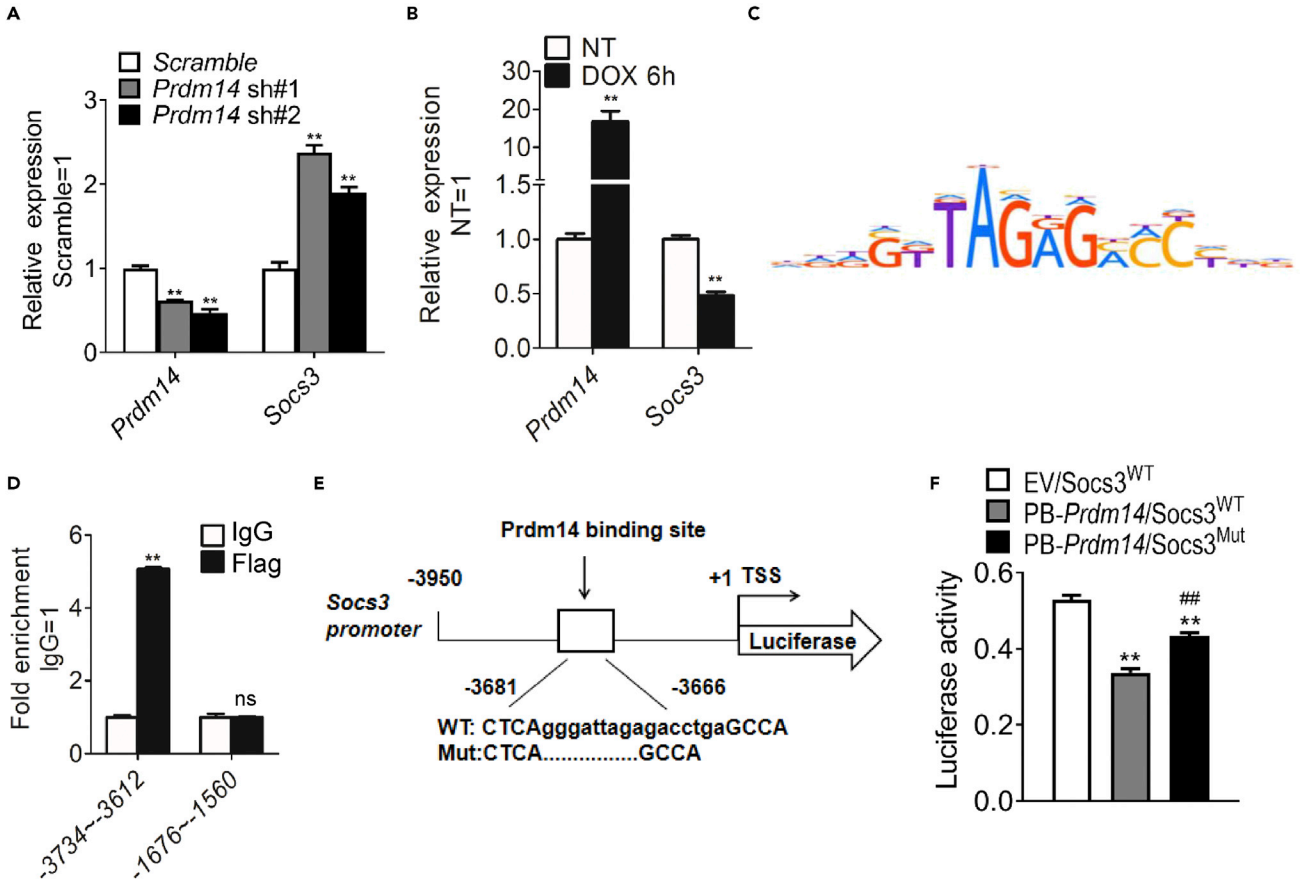

Figure 4. *Prdm14* directly inhibits the expression of *Socs3*

(A) qRT−PCR analysis of *Prdm14* and *Socs3* expression in 46C mESCs infected with *scramble* or *Prdm14* shRNA lentiviruses. The data are presented as the mean ± SD (N = 3 biological replicates). **p < 0.01 versus scramble, as determined by one-way ANOVA with Dunnet's multiple comparisons test.

(B) qRT−PCR analysis of *Prdm14* and *Socs3* transcripts in i-*Prdm14* cells treated with or without Dox for 6 h. The data are presented as the mean ± SD (N = 3 biological replicates). **p < 0.01 versus NT, as determined by one-way ANOVA with Dunnet's multiple comparisons test.

(C) The consensus binding motif of *Prdm14* predicted by the HOCOMOCO database.

(D) ChIP assays were performed using a Flag antibody. IgG was used as a negative control. The fold enrichment in the indicated regions of the Socs3 promoter was measured by qRT−PCR. The data are presented as the mean ± SD (N = 3 biological replicates). **p < 0.01 versus IgG, as determined by Student's *t* test. ns: nonsignificant.

(E) The binding position and sequence of Prdm14 in the Socs3 promoter and the corresponding deletion mutation sequence. *TSS*, transcription start site.

(F) Luciferase activity analysis of the wild-type (WT) or mutant (Mut) Socs3 promoter reporter plasmid-expressing cell lines transfected with or without PB-*Prdm14*. The data are presented as the mean ± SD (N = 3 biological replicates). **p < 0.01 versus EV/Socs3^{WT}, $^{\#\#}$p < 0.01 versus PB-*Prdm14*/*Socs3*^{WT}, as determined by one-way ANOVA with Sidak's multiple comparisons test.

See also Figures S6–S8 and Tables S2–S4.

formation. First, we established three mESC lines expressing EV, PB-*Prdm14*, or PB-*Prdm14*/PB-*Socs3*, in which *Prdm14* and *Sosc3* were efficiently induced (Figures 5A, S9A, and S9B). ESCs were first converted into EpiLCs and then incubated in KSR-containing medium in the presence or absence of the inductive cytokines BMP4, LIF, SCF, and EGF for 4 days. Immunofluorescence staining of *Tfap2c* showed that overexpression of *Socs3* reduced the efficiency of Prdm14 in inducing PGCLC specification (Figure 5B). Next, we used a mouse ESC cell line in which the expression of the EGFP gene was driven by a fragment of mouse Blimp1 promoter (Zhang et al., 2021). Similar results could be observed in sorting *Blimp1*-positive cells by fluorescence-activated cell sorting (FACS) (Figure 5C). Moreover, qRT−PCR analysis showed that overexpression of *Prdm14* increased the efficiency of PGCLC generation compared with control *EV* (Figure 5D), while enforced expression of *Socs3* decreased the expression levels of the PGCLC markers *Blimp1*, *Nanos3*, and *Tfap2c* induced by *Prdm14* in the presence of inductive cytokines (Figure 5D). Since upregulation of *Prdm14* alone is sufficient for the induction of PGCLCs from EpiLCs without cytokines (Figure 5E) (Nakaki et al., 2013), we finally wanted to confirm the negative function of Socs3 on the effect of Prdm14 in

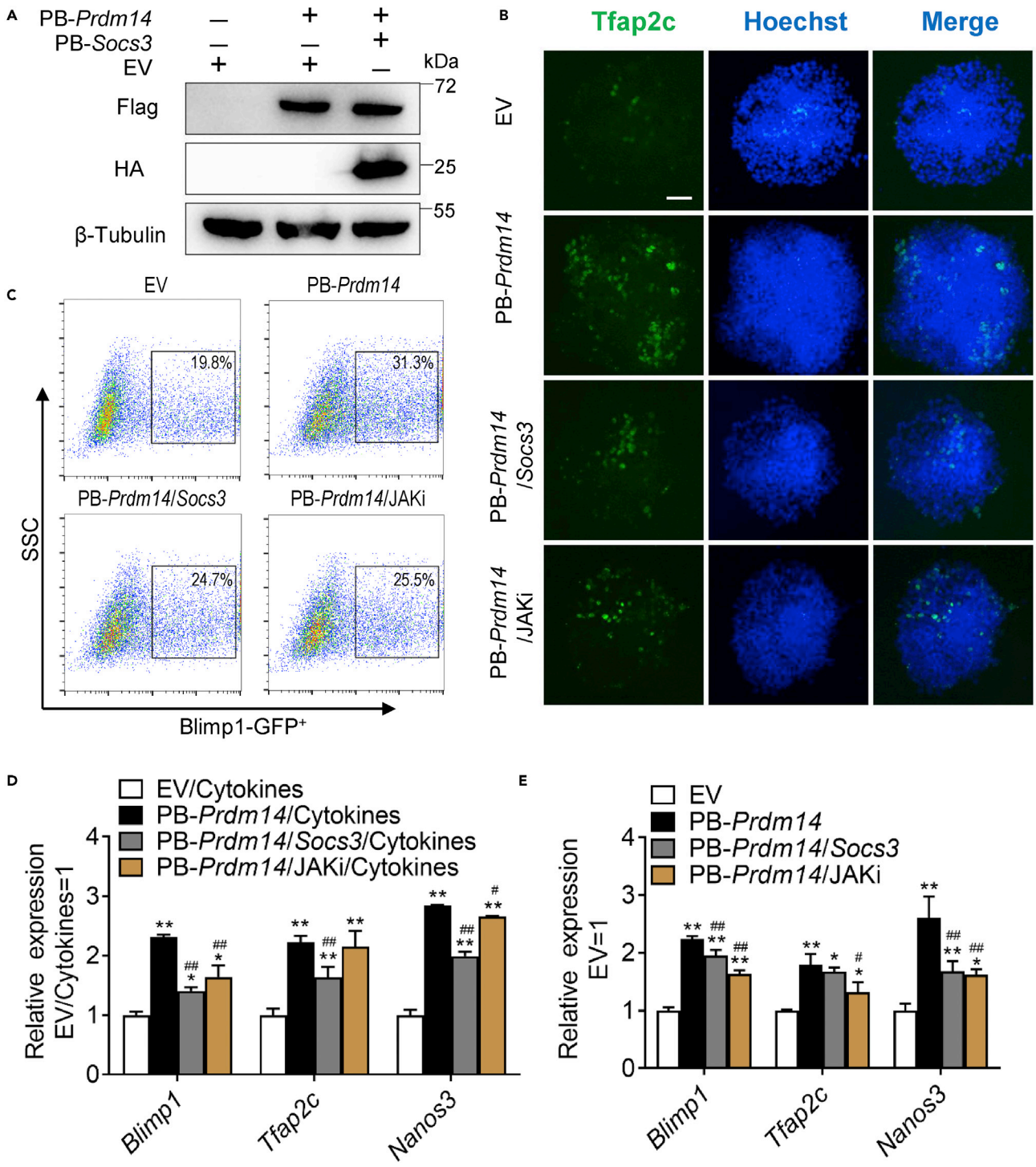

Figure 5. Inhibition of LIF/Stat3 signaling decreases PGCLC markers induced by *Prdm14* overexpression

(A) Western blot analysis of Flag and HA in EV-, *Prdm14*-, and *Prdm14*/*Socs3*-expressing 46C mESCs. β-Tubulin was used as a loading control.

(B) Immunofluorescence staining of PGCLC marker gene Tfap2c in EV- and *Prdm14*-expressing PGCLCs transfected with *Socs3* or treated with 5 μM JAKi in the presence of cytokines. Bar,100 μM.

(C) The FACS profile for Blimp1-positive PGCLCs on Day 4.

(D) qRT−PCR analysis of the expression of *Blimp1*, *Tfap2c* and *Nanos3* in EV- and *Prdm14*-expressing PGCLCs transfected with *Socs3* or treated with 5 μM JAKi in the presence of the cytokines BMP4, LIF, SCF, and EGF. The data are presented as the mean ± SD (N = 3 biological replicates). *$p < 0.05$, **$p < 0.01$ versus EV/cytokines, $^{\#}p < 0.05$, $^{\#\#}p < 0.01$ versus PB-*Prdm14*/cytokines, as determined by one-way ANOVA with Sidak's multiple comparisons test.

Figure 5. *Continued*

(E) qRT−PCR analysis of the expression of the *Blimp1*, *Tfap2c* and *Nanos3* in EV- and *Prdm14*-expressing PGCLCs transfected with *Socs3* or treated with 5 μM JAKi in the absence of cytokines. The data are presented as the mean ± SD (N = 3 biological replicates). *p < 0.05, **p < 0.01 versus EV, $^{\#}$p < 0.05, $^{\#\#}$p < 0.01 versus PB-*Prdm14*, as determined by one-way ANOVA with Sidak's multiple comparisons test.

See also Figure S9 and Table S3.

promoting PGCLC formation. As expected, upregulation of *Socs3* was able to reduce the transcripts of PGC markers maintained by *Prdm14* (Figure 5E). Notably, the addition of JAK inhibitor I had weaker effects than *Socs3* overexpression on *Prdm14*-induced PGCLC specification in the presence of PGC-inductive cytokines (Figure 5D). However, they have similar inhibitory effects in the absence of PGC-inductive cytokines (Figure 5E). Taken together, these results indicate that overexpression of *Socs3* does not facilitate the generation of PGCLCs induced by Prdm14.

DISCUSSION

As a master regulator of pluripotency maintenance and PGCLC acquisition, the systematic and specific mechanism of Prdm14 is still unknown. We revealed that Prdm14 functions partially through augmenting the activity of the LIF/Stat3 signaling pathway by directly suppressing the transcription of *Socs3*. Ectopic expression of *Socs3* is able to impair the function of *Prdm14* in promoting mESC self-renewal and inducing PGCLC formation. These results reveal how a germ-cell-specific gene interacts with pluripotency-associated signaling pathways to sustain ESC stemness and induce PGC specification.

Socs3 is a key bridge connecting Prdm14 and the LIF/Stat3 signaling pathway in pluripotent stem cells, and the mechanism can be explained as follows. First, although *Socs3* is a direct target gene of LIF/Stat3 signaling, the dramatic upregulation of *Socs3* in different tissues strongly inhibits the activity of Stat3 via binding with JAK2 and Gp130, both of which are positive upstream modulators of Stat3 activity (Kershaw et al., 2013; Sasaki et al., 1999; Schmitz et al., 2000). Second, elevation of *Socs3* is not beneficial for self-renewal but favors differentiation of mESCs (Chambers and Smith, 2004; Li et al., 2005). Therefore, inhibition of *Socs3* promotes the maintenance of mESC identity (Figures 3C and 3D). Similar results have also been observed in porcine-induced pluripotent stem cells, in which the expression of Socs3 is tightly controlled by METTL3-mediated N6-methyladenosine methylation (Wu et al., 2019). Loss of *METTL3* significantly impairs self-renewal and triggers differentiation by enhancing *Socs3* expression (Wu et al., 2019). Of note, in addition to Prdm14, a previous study also observed that *Nanog*, a core pluripotent gene can amplify Stat3 activation by suppressing *Socs3* to induce naive pluripotency (Stuart et al., 2014). These results enrich our understanding of the regulatory network around Socs3 to help study the regulation of ESC pluripotency.

Prdm14 shares many features with the LIF/Stat3 signaling pathway in stem cell self-renewal maintenance, pluripotency induction, and PGC acquisition. For example, constitutive expression of *Prdm14* or *Stat3* can confer LIF independence to maintain the undifferentiated state (Niwa et al., 1998; Okashita et al., 2015). Furthermore, overexpression of *Prdm14* together with *Klf2* is able to accelerate and enhance the reversion of mouse epiblast stem cells to a naive pluripotent state even in the absence of LIF (Gillich et al., 2012; Okashita et al., 2016). Activation of Stat3 also has the ability to convert epiblast stem cells into chimera-competent pluripotent stem cells (Yang et al., 2010). Additionally, overexpression of *Prdm14* promotes PGCLC specification in epiblast-like cells without LIF supplementation (Nakaki et al., 2013); the latter is an important cytokine for inducing PGCLC generation (Hayashi et al., 2011). However, the mechanisms contributing to the action of Prdm14 and LIF/Stat3 signaling may be different. Prdm14 safeguards mESC maintenance by preventing the emergence of extraembryonic endoderm fate and an epiblast-like state (Ma et al., 2011; Yamaji et al., 2013), whereas LIF/Stat3 signaling constrains the mesodermal and endodermal commitment (Ying et al., 2003). On the other hand, *Prdm14* alone suffices for the induction of the PGC state (Nakaki et al., 2013), while LIF has to work with BMP4 (Hayashi et al., 2011). Additionally, *Prdm14* is downstream of Stat3 but is not a direct target of Stat3 (Figure 3A). These data indicate that the relationship between Prdm14 and LIF/Stat3 signaling is very complex and requires further exploration.

A previous study showed that *Prdm14* exerts its effects by recruiting SUZ12 and JARID2; the former is a component of PRC2, and the latter is able to recruit PRC2 to target loci to repress gene expression by inducing H3K27me3 (Yamaji et al., 2013). We also demonstrated H3K27me3 enrichment at the Socs3 promoter regions when *Prdm14* was overexpressed (Figures S8A and S8B), suggesting that the PRC2 complex may be responsible for the effect of *Prdm14* on *Socs3* transcription. In addition, Prdm14 is also thought to be closely associated with Dnmt3a/b/l repression and Tet recruitment at target loci, leading to the

activation of Akt-mTOR signaling and the inactivation of Fgf/Erk signaling to ensure global DNA hypomethylation in mESCs and PGCs (Okashita et al., 2014; Yamaji et al., 2013). Whether this epigenetic regulation mechanism is involved in the inhibitory effect of Prdm14 on *Socs3* transcription needs to be further investigated.

Limitations of the study

There were several limitations to the present study. First, Prdm14 and LIF/Stat3 signals have a mutual feedback function. However, we did not analyze this regulatory mechanism in detail. Second, we did not evaluate the function of Prdm14 during *Stat3*-mediated primed stem cell reprogramming. Finally, which component of PRC2 is incorporated by Prdm14 to promote the occurrence of H3K27me3 and further inhibit the expression of Socs3 has not yet been identified.

In summary, our study provides more mechanistic insight into the function of Prdm14 in ESCs and the development of PGC specification. For the first time, our findings suggest that Prdm14 amplifies LIF/Stat3 signaling by directly suppressing *Socs3* expression. Identifying the relationship between Prdm14 and Stat3 activity will facilitate a better understanding of the regulatory circuitry of the maintenance of naive pluripotency and specification of germ cells.

STAR★METHODS

Detailed methods are provided in the online version of this paper and include the following:

- KEY RESOURCES TABLE
- RESOURCE AVAILABILITY
  - Lead contact
  - Materials availability
  - Data and code availability
- EXPERIMENTAL MODEL AND SUBJECT DETAILS
  - Cell lines
- METHOD DETAILS
  - Plasmid construction
  - AP activity assay
  - Western blot analysis
  - qRT−PCR
  - Immunofluorescence staining
  - ChIP assay
  - Luciferase assay
  - Mouse PGCLC induction
  - Cell transfection and infection
- QUANTIFICATION AND STATISTICAL ANALYSIS
  - Statistics

SUPPLEMENTAL INFORMATION

Supplemental information can be found online at https://doi.org/10.1016/j.isci.2022.105293.

ACKNOWLEDGMENTS

This work was supported by the Natural Science Foundation of Anhui Province [1908085J13], the Anhui Provincial Key Research and Development Plan [202104b11020026], the University Synergy Innovation Program of Anhui Province [GXXT-2020-064], the Funding supported by the Department of Education of Anhui Province and the Department of Human Resources and Social Security of Anhui Province [gxyqZD2020001 and 2020H210], the Innovation Projects for College Students [YJS20210041 and S202110357122] and the research funding of USTC [2019ZC006].

AUTHOR CONTRIBUTIONS

Conceptualization, Y.T.L. and Z.Q.Y.; Investigation, Y.T.L., Z.Q.Y., and X.F.L.; Methodology, X.X.W.; Formal Analysis and Resources, Y.Y., X.F.L., P.C., and B.L.; Supervision, SD.Y.; Writing – Original Draft, Y.T.L.; Writing –Review & Editing, X.X.W. and SD.Y.

DECLARATION OF INTERESTS

The authors declare no competing interests.

Received: October 26, 2021
Revised: July 13, 2022
Accepted: October 3, 2022
Published: November 18, 2022

REFERENCES

Babon, J.J., Kershaw, N.J., Murphy, J.M., Varghese, L.N., Laktyushin, A., Young, S.N., Lucet, I.S., Norton, R.S., and Nicola, N.A. (2012). Suppression of cytokine signaling by SOCS3: characterization of the mode of inhibition and the basis of its specificity. Immunity *36*, 239–250. https://doi.org/10.1016/j.immuni.2011.12.015.

Chambers, I., and Smith, A. (2004). Self-renewal of teratocarcinoma and embryonic stem cells. Oncogene *23*, 7150–7160. https://doi.org/10.1038/sj.onc.1207930.

Evans, M.J., and Kaufman, M.H. (1981). Establishment in culture of pluripotential cells from mouse embryos. Nature *292*, 154–156. https://doi.org/10.1038/292154a0.

Gillich, A., Bao, S., Grabole, N., Hayashi, K., Trotter, M.W., Pasque, V., Magnusdottir, E., and Surani, M.A. (2012). Epiblast stem cell-based system reveals reprogramming synergy of germline factors. Cell Stem Cell *10*, 425–439. https://doi.org/10.1016/j.stem.2012.01.020.

Hall, J., Guo, G., Wray, J., Eyres, I., Nichols, J., Grotewold, L., Morfopoulou, S., Humphreys, P., Mansfield, W., Walker, R., et al. (2009). Oct4 and LIF/Stat3 additively induce Kruppel factors to sustain embryonic stem cell self-renewal. Cell Stem Cell *5*, 597–609. https://doi.org/10.1016/j.stem.2009.11.003.

Hayashi, K., Ohta, H., Kurimoto, K., Aramaki, S., and Saitou, M. (2011). Reconstitution of the mouse germ cell specification pathway in culture by pluripotent stem cells. Cell *146*, 519–532. https://doi.org/10.1016/j.cell.2011.06.052.

Huang, G., Ye, S., Zhou, X., Liu, D., and Ying, Q.L. (2015). Molecular basis of embryonic stem cell self-renewal: from signaling pathways to pluripotency network. Cell. Mol. Life Sci. *72*, 1741–1757. https://doi.org/10.1007/s00018-015-1833-2.

Kershaw, N.J., Murphy, J.M., Liau, N.P., Varghese, L.N., Laktyushin, A., Whitlock, E.L., Lucet, I.S., Nicola, N.A., and Babon, J.J. (2013). SOCS3 binds specific receptor-JAK complexes to control cytokine signaling by direct kinase inhibition. Nat. Struct. Mol. Biol. *20*, 469–476. https://doi.org/10.1038/nsmb.2519.

Kulakovskiy, I.V., Vorontsov, I.E., Yevshin, I.S., Sharipov, R.N., Fedorova, A.D., Rumynskiy, E.I., Medvedeva, Y.A., Magana-Mora, A., Bajic, V.B., Papatsenko, D.A., et al. (2018). HOCOMOCO: towards a complete collection of transcription factor binding models for human and mouse via large-scale ChIP-Seq analysis. Nucleic Acids Res. *46*, D252–D259. https://doi.org/10.1093/nar/gkx1106.

Li, Y., McClintick, J., Zhong, L., Edenberg, H.J., Yoder, M.C., and Chan, R.J. (2005). Murine embryonic stem cell differentiation is promoted by SOCS-3 and inhibited by the zinc finger transcription factor Klf4. Blood *105*, 635–637. https://doi.org/10.1182/blood-2004-07-2681.

Ma, Z., Swigut, T., Valouev, A., Rada-Iglesias, A., and Wysocka, J. (2011). Sequence-specific regulator Prdm14 safeguards mouse ESCs from entering extraembryonic endoderm fates. Nat. Struct. Mol. Biol. *18*, 120–127. https://doi.org/10.1038/nsmb.2000.

Margueron, R., and Reinberg, D. (2011). The Polycomb complex PRC2 and its mark in life. Nature *469*, 343–349. https://doi.org/10.1038/nature09784.

Martello, G., Bertone, P., and Smith, A. (2013). Identification of the missing pluripotency mediator downstream of leukaemia inhibitory factor. EMBO J. *32*, 2561–2574. https://doi.org/10.1038/emboj.2013.177.

Martin, G.R. (1981). Isolation of a pluripotent cell line from early mouse embryos cultured in medium conditioned by teratocarcinoma stem cells. Proc. Natl. Acad. Sci. USA *78*, 7634–7638. https://doi.org/10.1073/pnas.78.12.7634.

Nady, N., Gupta, A., Ma, Z., Swigut, T., Koide, A., Koide, S., and Wysocka, J. (2015). ETO family protein Mtgr1 mediates Prdm14 functions in stem cell maintenance and primordial germ cell formation. Elife *4*, e10150. https://doi.org/10.7554/eLife.10150.

Nakaki, F., Hayashi, K., Ohta, H., Kurimoto, K., Yabuta, Y., and Saitou, M. (2013). Induction of mouse germ-cell fate by transcription factors in vitro. Nature *501*, 222–226. https://doi.org/10.1038/nature12417.

Niwa, H., Burdon, T., Chambers, I., and Smith, A. (1998). Self-renewal of pluripotent embryonic stem cells is mediated via activation of STAT3. Genes Dev. *12*, 2048–2060. https://doi.org/10.1101/gad.12.13.2048.

Okashita, N., Kumaki, Y., Ebi, K., Nishi, M., Okamoto, Y., Nakayama, M., Hashimoto, S., Nakamura, T., Sugasawa, K., Kojima, N., et al. (2014). PRDM14 promotes active DNA demethylation through the ten-eleven translocation (TET)-mediated base excision repair pathway in embryonic stem cells. Development *141*, 269–280. https://doi.org/10.1242/dev.099622.

Okashita, N., Sakashita, N., Ito, K., Mitsuya, A., Suwa, Y., and Seki, Y. (2015). PRDM14 maintains pluripotency of embryonic stem cells through TET-mediated active DNA demethylation. Biochem. Biophys. Res. Commun. *466*, 138–145. https://doi.org/10.1016/j.bbrc.2015.08.122.

Okashita, N., Suwa, Y., Nishimura, O., Sakashita, N., Kadota, M., Nagamatsu, G., Kawaguchi, M., Kashida, H., Nakajima, A., Tachibana, M., et al. (2016). PRDM14 drives OCT3/4 recruitment via active demethylation in the transition from primed to naive pluripotency. Stem Cell Rep. *7*, 1072–1086. https://doi.org/10.1016/j.stemcr.2016.10.007.

Sasaki, A., Yasukawa, H., Suzuki, A., Kamizono, S., Syoda, T., Kinjyo, I., Sasaki, M., Johnston, J.A., and Yoshimura, A. (1999). Cytokine-inducible SH2 protein-3 (CIS3/SOCS3) inhibits Janus tyrosine kinase by binding through the N-terminal kinase inhibitory region as well as SH2 domain. Gene Cell. *4*, 339–351. https://doi.org/10.1046/j.1365-2443.1999.00263.x.

Schmitz, J., Weissenbach, M., Haan, S., Heinrich, P.C., and Schaper, F. (2000). SOCS3 exerts its inhibitory function on interleukin-6 signal transduction through the SHP2 recruitment site of gp130. J. Biol. Chem. *275*, 12848–12856. https://doi.org/10.1074/jbc.275.17.12848.

Sim, Y.J., Kim, M.S., Nayfeh, A., Yun, Y.J., Kim, S.J., Park, K.T., Kim, C.H., and Kim, K.S. (2017). 2i maintains a naive ground state in ESCs through two distinct epigenetic mechanisms. Stem Cell Rep. *8*, 1312–1328. https://doi.org/10.1016/j.stemcr.2017.04.001.

Smith, A.G., Heath, J.K., Donaldson, D.D., Wong, G.G., Moreau, J., Stahl, M., and Rogers, D. (1988). Inhibition of pluripotential embryonic stem cell differentiation by purified polypeptides. Nature *336*, 688–690. https://doi.org/10.1038/336688a0.

Stuart, H.T., van Oosten, A.L., Radzisheuskaya, A., Martello, G., Miller, A., Dietmann, S., Nichols, J., and Silva, J.C. (2014). NANOG amplifies STAT3 activation and they synergistically induce the naive pluripotent program. Curr. Biol. *24*, 340–346. https://doi.org/10.1016/j.cub.2013.12.040.

Tai, C.I., and Ying, Q.L. (2013). Gbx2, a LIF/Stat3 target, promotes reprogramming to and retention of the pluripotent ground state. J. Cell Sci. *126*, 1093–1098. https://doi.org/10.1242/jcs.118273.

Williams, R.L., Hilton, D.J., Pease, S., Willson, T.A., Stewart, C.L., Gearing, D.P., Wagner, E.F., Metcalf, D., Nicola, N.A., and Gough, N.M. (1988). Myeloid leukaemia inhibitory factor maintains the developmental potential of embryonic stem cells. Nature *336*, 684–687. https://doi.org/10.1038/336684a0.

Wu, R., Liu, Y., Zhao, Y., Bi, Z., Yao, Y., Liu, Q., Wang, F., Wang, Y., and Wang, X. (2019). m(6)A

methylation controls pluripotency of porcine induced pluripotent stem cells by targeting SOCS3/JAK2/STAT3 pathway in a YTHDF1/YTHDF2-orchestrated manner. Cell Death Dis. *10*, 171. https://doi.org/10.1038/s41419-019-1417-4.

Yamaji, M., Seki, Y., Kurimoto, K., Yabuta, Y., Yuasa, M., Shigeta, M., Yamanaka, K., Ohinata, Y., and Saitou, M. (2008). Critical function of Prdm14 for the establishment of the germ cell lineage in mice. Nat. Genet. *40*, 1016–1022. https://doi.org/10.1038/ng.186.

Yamaji, M., Ueda, J., Hayashi, K., Ohta, H., Yabuta, Y., Kurimoto, K., Nakato, R., Yamada, Y., Shirahige, K., and Saitou, M. (2013). PRDM14 ensures naive pluripotency through dual regulation of signaling and epigenetic pathways in mouse embryonic stem cells. Cell Stem Cell *12*, 368–382. https://doi.org/10.1016/j.stem.2012.12.012.

Yang, J., van Oosten, A.L., Theunissen, T.W., Guo, G., Silva, J.C., and Smith, A. (2010). Stat3 activation is limiting for reprogramming to ground state pluripotency. Cell Stem Cell *7*, 319–328. https://doi.org/10.1016/j.stem.2010.06.022.

Ye, S., Li, P., Tong, C., and Ying, Q.L. (2013). Embryonic stem cell self-renewal pathways converge on the transcription factor Tfcp2l1. EMBO J. *32*, 2548–2560. https://doi.org/10.1038/emboj.2013.175.

Ye, S., Zhang, D., Cheng, F., Wilson, D., Mackay, J., He, K., Ban, Q., Lv, F., Huang, S., Liu, D., et al. (2016). Wnt/beta-catenin and LIF-Stat3 signaling pathways converge on Sp5 to promote mouse embryonic stem cell self-renewal. J. Cell Sci. *129*, 269–276. https://doi.org/10.1242/jcs.177675.

Ying, Q.L., Nichols, J., Chambers, I., and Smith, A. (2003). BMP induction of Id proteins suppresses differentiation and sustains embryonic stem cell self-renewal in collaboration with STAT3. Cell *115*, 281–292. https://doi.org/10.1016/s0092-8674(03)00847-x.

Zhang, M., Ji, J., Wang, X., Zhang, X., Zhang, Y., Li, Y., Wang, X., Li, X., Ban, Q., and Ye, S.D. (2021). The transcription factor Tfcp2l1 promotes primordial germ cell-like cell specification of pluripotent stem cells. J. Biol. Chem. *297*, 101217. https://doi.org/10.1016/j.jbc.2021.101217.

STAR★METHODS

KEY RESOURCES TABLE

REAGENT or RESOURCE	SOURCE	IDENTIFIER
Antibodies		
FLAG	GNI	Cat#GNI4110-FG-S
FLAG	Sigma-Aldrich	Cat#F1804, RRID:AB_262044
HA	GNI	Cat#GNI4110-HA-S
Prdm14	BBI, China	Cat#D221722
Socs3	Santa Cruz	Cat# sc-73045, RRID:AB_1129585
Stat3	Cell Signaling Technology	Cat#12640, RRID:AB_2629499
phospho-Stat3^{Y705}	Cell Signaling Technology	Cat#9131, RRID:AB_331586
H3K27me3	Active Motif	Cat#39055 RRID:AB_2561020
H3	Cell Signaling Technology	Cat#4620, RRID:AB_1904005
β-Tubulin	Zen Bioscience, China	Cat# 200608, RRID:AB_2722706
HRP Goat Anti-Mouse IgG (H + L)	Abclonal, China	Cat#AS003, RRID:AB_2769851
HRP Goat Anti-Rabbit IgG (H + L)	Abclonal, China	Cat#AS014, RRID:AB_2769854
Sox2	ProteinTech	Cat# 66411-1-Ig, RRID:AB_2881783
Tfap2c	Santa Cruz	Cat# sc-12762 RRID:AB_667770
Chemicals, peptides, and recombinant proteins		
JAK Inhibitor I	Santa Cruz	Cat# sc-204021
LIF	Millipore	Cat# LIF1010
AgeI	NEB	Cat# R0552S
EcoRI	NEB	Cat# R0101S
PCR polymerase	Vazyme, China	Cat# P502-d1
T4 DNA Ligase	Monad, China	Cat# MC00102M
Puromycin	YEASEN, China	Cat#60210ES25
Blasticidin S	YEASEN, China	Cat#60218ES0
Paraformaldehyde	Sigma	Cat#V900894
Albumin Bovine	Biosharp, China	Cat#BS114-250g
Hoechst 33342	Invitrogen	Cat#H3570
Fibronectin	Sigma	Cat#F1141-5MG
KSR	Invitrogen	Cat#10828028
BMP4	Peprotech	Cat#315-27-10
SCF	Peprotech	Cat#AF-250-03
EGF	Peprotech	Cat#AF-100-15
GMEM	Gibico	Cat#11710035
CHIR99021	MedChemExpress, China	Cat# HY-10182
PD0325901	ApexBio	Cat# A3013
Activin A	Novoprotein	Cat# C678
bFGF	Novoprotein	Cat# C044

(*Continued on next page*)

Continued

REAGENT or RESOURCE	SOURCE	IDENTIFIER
BglII	Monad, China	Cat#MF03301S
XhoI	Monad, China	Cat#MF03001S
SalI	Monad, China	Cat#MF02201M
BamHI	Monad, China	Cat#MF00201S
KpnI	Takara, China	Cat#1618
BclI	Takara, China	Cat#1045A
DMEM, high glucose	Biological Industries, Israel	Cat#2122149
Fetal bovine serum	ExCell Bio, Australia	Cat#FND500
MEM nonessential amino acids	Solarbio	Cat#N1250
β-mercaptoethanol	Sigma	Cat# M3148
sodium pyruvate	Solarbio	Cat#SP0100
Trypsin-EDTA	Biosharp, China	Cat#BL501A
ECL reagent	Tanon, China	Cat#180-501
RIPA	Beyotime Biotechnology, China	Cat# P0013B
3M NaAc, pH 5.2	Beyotime Biotechnology, China	Cat#ST351
Glycogen	Beyotime Biotechnology, China	Cat#D0812
Proteinase K	Beyotime Biotechnology, China	Cat#ST533
Doxycycline hyclate	ApexBio	Cat#A4052
Protease Inhibitor Cocktail	ApexBio	Cat#K1007
PVDF membranes	Sangon Biotech, China	Cat#F619537-0001
10×PBS	Biosharp, China	Cat#BL316A
NaCl	Sinopharm, China	Cat#10019318
Triton™ X-100	Sigma	Cat#T8787
Critical commercial assays		
SDS-PAGE Color Preparation kit	Sangon Biotech, China	Cat#C671102-0125
AP staining kit	Beyotime Biotechnology, China	Cat#C3206
ChIP Assay Kit	Beyotime Biotechnology, China	Cat#P2078
TransDetect® Double-Luciferase Reporter Assay Kit	Trans-Gen Biotech, China	Cat#FR201
RNAeasy™ Animal RNA Isolation Kit with Spin Column	Beyotime, China	Cat# R0027
Reverse Transcription Kit (with dsDNase)	Biosharp, China	Cat#BL699A
Universal SYBR qPCR Master Mix	Biosharp, China	Cat#BL697A
TIANprep Mini Plasmid Kit	TIANGEN, China	Cat#DP103-03
TIANquick Midi Purification Kit	TIANGEN, China	Cat#DP204-03
TIANgel Midi Purification Kit	TIANGEN, China	Cat#DP209-03
Experimental models: Cell lines		
46C mESCs	PMID: 12524553	N/A
293FT	Thermo Fisher	Cat#R70007
Oligonucleotides		
Prdm14 sh#1: ACCTTGAATTACAGGATTAAG	This Study	N/A
Prdm14 sh#2: TTAAGTCGTCCCAGTCAATAT	This Study	N/A

(*Continued on next page*)

Continued

REAGENT or RESOURCE	SOURCE	IDENTIFIER
Stat3 sh#1: CCTGAGTTGAATTATCAGCTT	This Study	N/A
Stat3 sh#2: CCTAACTTTGTGGTTCCAGAT	This Study	N/A
Socs3 sh#1: GATCAGTATGATGCTCCACTT	This Study	N/A
Socs3 sh#2: GCTAGGAGACTCGCCTTAAAT	This Study	N/A
Additional Primer sequences are provided in Table S3	This Study	N/A
Recombinant DNA		
PB-Flag-*Prdm14*	This study	N/A
PB-HA-*Socs3*	This study	N/A
PB-Teton-*Prdm14*	This study	N/A
pLKO.1 *Prdm14* sh#1	This study	N/A
pLKO.1 *Prdm14* sh#2	This study	N/A
pLKO.1 *Stat3* sh#1	This study	N/A
pLKO.1 *Stat3* sh#2	This study	N/A
pLKO.1 *Socs3* sh#1	This study	N/A
pLKO.1 *Socs3* sh#2	This study	N/A
Software and algorithms		
ImageJ	https://imagej.nih.gov/ij/	https://imagej.nih.gov/ij/RRID: SCR_003070
Endnote X9	Endnote X9.3.2 (Bld 15235)	endnote.com
GraphPad Prism	Version 8.4.0 (455), February 20, 2020	https://www.graphpad.com, RRID:SCR_002798
Primer3	https://primer3.org/	https://primer3.org/
Primer Premier 5	Premier	https://www.bioprocessonline.com/doc/primer-premier-5-design-program-0001
DNAMAN	LynnonBiosoft	www.lynnon.com/dnaman.html
Other		
pLKO.1-TRC	Addgene	Cat#10878, RRID:Addgene_10878
PB-Tetone-MCS-puro	This study	N/A
PGL6	Beyotime Biotechnology, China	Cat# D2102
Penicillin-Streptomycin Liquid	Solarbio, China	Cat# P1400
Hieff Trans™ Liposomal Transfection Reagent	YEASEN, China	Cat# 40802ES03
Fetal bovine serum	CLARK Bioscience	Cat# FB25015
Ampicillin sodium	BBI, China	Cat# A610028
Agarose	YEASEN, China	Cat# 10208ES60

RESOURCE AVAILABILITY

Lead contact

Further information and requests for resources and reagents should be directed to and will be fulfilled by the lead contact Shou-Dong Ye, (shdye@126.com).

Materials availability

In this work, the newly generated material was represented by mammalian expression plasmids. All these plasmids are listed in the key resources table and can be shared upon request.

Data and code availability

- Our transcriptome sequencing data has been deposited in the GEO database with the accession number GSE184802.
- This paper does not report original code.
- Any additional information required to reanalyze the data reported in this paper is available from the lead contact upon request.

EXPERIMENTAL MODEL AND SUBJECT DETAILS

Cell lines

46C mESCs, kindly provided by Qi-Long Ying (University of Southern California, USA), were cultured in 0.1% gelatin-coated dishes at 37°C in 5% carbon dioxide. The medium used for routine maintenance was DMEM (Biological Industries, Israel) supplemented with 15% FBS (FND500, ExCell Bio, Australia), 1× MEM nonessential amino acids (N1250, Solarbio, China), 0.1 mM β-mercaptoethanol (M3148, Sigma) and 1000 U/ml LIF (LIF1010, Millipore, USA). Cells were digested by 0.05% Trypsin-EDTA solution every 2–3 days.

METHOD DETAILS

Plasmid construction

The coding regions of mouse *Prdm14* and *Socs3* were inserted into PiggyBac transposon vectors (PB) carrying Flag or HA tag. shRNA sequences, designed to target the gene-specific regions of mouse *Prdm14*, *Socs3* and *Stat3*, were cloned into pLKO.1-TRC vector (#10878, Addgene). The primer sequences used have been listed in Tables S1 and S2.

AP activity assay

Cells were fixed with 4% paraformaldehyde at room temperature for 2 min. After washing twice with PBS, cells were incubated in AP staining reagent (C3206, Beyotime Biotechnology, China) for 30 min at room temperature in the darkroom. Cells were observed under the Leica DMI8 microscope.

Western blot analysis

Cells were lysed in ice-cold RIPA cell buffer (P0013B, Beyotime Biotechnology, China) supplemented with protease inhibitor cocktail. The proteins (40–100 μg) were separated on 10–15% PAGE gels and electrotransferred onto polyvinylidene fluoride membranes. After blocking with 5% skimmed milk, the membrane was incubated with specific primary antibody and horseradish peroxidase-conjugated secondary antibody. The antibodies used are Flag (GNI4110-FG-S, GNI, Japan, 1:1000), HA (GNI4110-HA-S, GNI, Japan, 1:1000), Stat3 (12640S, Cell Signaling Technology, USA,1:1000), phospho-Stat3^{Y705} (9131S, Cell Signaling Technology, USA, 1:1000), Socs3 (sc-73045, Santa Cruz, 1:1000), Prdm14(D221722, BBI, China, 1:1000), H3K27me3 (39055, Active Motif, China, 1:1000), H3 (4620s,Cell Signaling Technology, USA, 1:1000) and β-Tubulin (200608, ZENBIO, China, 1:2000). The band density was analyzed with ImageJ according to ImageJ User Guide. Briefly, we inverted the greyscale images and select sample bands with rectangular selections. The proteins levels were normalized with respect to the β-Tubulin level, and the grayscale ratio of protein/β-Tubulin was calculated and visualized with GraphPad Prism 8.0.

qRT–PCR

Total RNA was extracted using RNAeasy Animal RNA Isolation Kit with Spin Column (R0027, Beyotime, China). cDNA was synthesized from 1 μg of total RNA with Reverse Transcription Kit (with dsDNase) (BL699A, Biosharp, China). qRT-PCR was carried out with Universal SYBR qPCR Master Mix (BL697A, Biosharp, China) in a PikoReal Real-Time PCR machine. The relative expression level was determined by the 2-ΔCq method and normalized to Rpl19 expression. The primers used are listed in Table S3.

Immunofluorescence staining

Cells were fixed in 4% paraformaldehyde for 30 min and then were incubated at 37°C for 2–3 h in blocking buffer (PBS containing 5% BSA and 0.2% Triton X-100). After washing three times with PBS, the cells were incubated with the primary antibody overnight at 4°C. After being washed three times with PBS, then the cells were incubated with the fluorescent secondary antibody and Hoechst 33342 (H3570, Invitrogen,

1:10000) for 1 h at 37°C in the darkroom. The cells were photographed under a Leica DMI8 microscope. The antibodies used are Sox2 (66411-1-Ig, Proteintech,1:500) and Tfap2c (sc-12762, Santa Cruz, 1:100).

ChIP assay

ChIP experiments were performed using a ChIP assay kit (P2078, Beyotime Biotechnology) according to the manufacturer's protocol. Flag antibody was used for immunoprecipitation and IgG was used as a negative control. ChIP enrichment was determined by qRT−PCR. The primer sequences and locations within the promoter regions of Socs3 are listed in Table S4.

Luciferase assay

The promoter sequence of Socs3 (from −3950 ∼ +20) was cloned into the pGL6 plasmid (pGL6-Socs3). The wild-type or mutant pGL6-Socs3 plasmids were cotransfected into 46C mESCs combined with Renilla luciferase plasmid and Prdm14-overexpressing construct. After 48 h, the luciferase activity was measured with a TransDetect® Double-Luciferase Reporter Assay Kit (FR201, Trans-Gen Biotech, China).

Mouse PGCLC induction

46C mESCs (3×10^5) were seeded in Fibronectin (16.7 μL/mL, F1141-5MG, Sigma) coated plates and cultured in N2B27 medium supplemented with 20 ng/mL Activin A (C678, Novoprotein, China), 12 ng/mL bFGF (C044, Novoprotein, China) and 1% KSR (10828028, Invitrogen) to induce epiblast like stem cells (EpiLCs). After two days, 2×10^5 EpiLCs were inoculated into GK15 medium for suspension culture for 4 days to induce PGCLCs in the presence of the inductive cytokines BMP4 (500 ng/mL, 315-27-10, Peprotech), LIF (1000 U/ml, Millipore), SCF (100 ng/mL, AF-250-03, Peprotech) and EGF (50 ng/mL, AF-100-15, Peprotech). GK15 consists of GMEM (11710035, Gibco), 15% KSR, 1×MEM nonessential amino acids, 0.1 mM β-mercaptoethanol and 1 mM sodium pyruvate (SP0100, Solarbio, China). After dissociation, the PGCLCs were resuspended in 1×PBS and analyzed on flow cytometers (FACS Calibur, BD Biosciences).

Cell transfection and infection

For gene overexpression, 2 μg of PB vectors and 2 μg of transposon plasmids were transfected into cells with Hieff Trans™ Liposomal Transfection Reagent (40802ES03, YEASEN, China) according to the manufacturer's instructions. For gene knockdown, 2 μg of pLKO.1, 0.75 μg of VSV-G and 1.25 μg of psPAX2 were cotransfected into 293FT cells. After 48 h of transfection, the virus supernatant was collected and added to the cell culture medium to infect the cells. The transfectants were selected by adding puromycin or blasticidin S HCl.

QUANTIFICATION AND STATISTICAL ANALYSIS

Statistics

The number of biological replicates is stated in each legend. All data are reported as the mean ± SD. Data were visualized with GraphPad Prism 8. Two paired Student's *t* test or one-way ANOVA with Sidak's or Dunnet's multiple comparisons test was used to determine the significance of differences in the following comparisons. $p < 0.05$ indicated statistical significance.